Supporting Information

Topology-Dependent Emissive Properties of Zirconium-Based Porphyrin MOFs

Pravas Deria,[,a] Jierui Yu,[a] Rajesh P. Balaraman,[a] Jamil Mashni,[a] and Sandra N. White[a,]*

[a] Department of Chemistry, Southern Illinois University, 1245 Lincoln Drive, Carbondale, Illinois 62901, United States.

Table of Contents

A. Materials

Solvents including acetone, *N,N*-dimethylformamide (DMF), diethyl ether, hexanes, and dichloromethane were purchased from Macron. DMF was filtered through activated basic alumina prior to MOF syntheses. *N,N'*-diethylformamide was received from Across Organics and used as received; propanoic acid, hydrochloric acid, sodium hydroxide were obtained from Fisher Scientific; deuterated $CDCl_3$ and dimethyl sulfoxide (dmso-d_6) (99%), and deuterated sulfuric acid (96-98% solution in D_2O) were obtained from Sigma-Aldrich and were used as received. Methyl *p*-formyl-benzoate was purchased from Combi-Blocks (San Diego, CA). Pyrrole was purchased from Sigma-Aldrich and was used as received.

B. Instrumentation

^{1}H NMR spectra were collected on a Varian Mercury plus 400 MHz instrument and were referenced to the residual solvent peak.

Powder X-ray diffraction (PXRD) patterns were recorded on a Rigaku Ultima IV diffractometer (measurements made over a range of $1.5° < 2\theta < 30°$ in 0.05° step width with a 2 deg/min scanning speed).

Scanning Electron Microscopy (SEM) and Energy Dispersive Spectroscopic (EDS) data were collected at Image Center, SIU Carbondale. Elemental analysis was performed using a Quanta FEG 450 Scanning Electron Microscope (SEM) equipped with an Oxford INCA Energy Dispersive Spectroscopy (EDS) system. Dried samples were spread on double-stick carbon tape on an aluminum SEM sample holder and was sputter–coated with Au and Pd using Denton Vacuum Desk III. Furthermore, the Fc-COO/por ratios were corroborated via ICP-MS data performed at Carbondale Central Laboratory, Carbondale, IL-62901.

Excitation spectra were recorded at room temperature using PTI fluorimeter. Samples for spectroscopic measurements were loaded inside the small capillary tube and sealed with grease inside a glovebox (Braun) under argon. Solid crystalline powder loaded capillary tubes were centrally-positioned inside a 3×3 mm quartz sample holder with fixed incident beam size and mounted in a front–face configuration. Spectra were then collected using a 2 nm excitation and 2 nm emission slit width, and excitation spectra were corrected using the instrumental correction function for the excitation light source.

Fluorescence lifetime emission decay profiles and time-resolved emission spectra were recorded using an Edinburg Lifespec II Picosecond Time-Correlated Single Photon Counting spectrophotometer equipped with Hamamatsu H10720-01 detector and a 405 nm picosecond pulsed diode laser as TCSPC source. Instrumental control, kinetic data collection, processing and fitting were performed using F980 software. This instrument displays a measured instrumental response function of 180 ps; as such, reconvolution based exponential fitting using F980 software was used to extract lifetime data as low as 20 ps ($1/10^{th}$ the instrument response function). Time resolved emission spectra (TRES) and slicing of the TRES data were also performed using F980 software.

C. Synthesis

C1. Synthesis of H_2TCPP[1]

Synthesis of TCPPOMe(H2):

Methyl p-formyl-benzoate 69.0 g (423 mmol) was dissolved in 100 mL of propionic acid in a 500 mL three-necked flask. Pyrrole 30 mL (432 mmol) was then added dropwise and the mixture was refluxed for 12h in dark. The purple crystalline precipitate was collected by filtration and washed with 50 mL of propionic acid followed by 100 mL of water. The precipitate was then dried under vacuum filtration at room temperature. Yield 18 g (20%); ^{1}H NMR (400 MHz, $CDCl_3$ as 7.26 ppm): δ 8.822 (s, 8H), 8.494 (d, 8H, J = 8.0 Hz), 8.296 (d, 8H, J = 8.0Hz), 4.115 (s, 12H), -2.825 (s, 2H). MS (MALDI-TOF): 846.39 [$M^{\bullet+}$] (calc 846).

Synthesis of TCPP(H2):

Potassium hydroxide 30.0 g (535 mmol) was dissolved in water (160 mL) and TPPCOOMe(H2) 15.0 g (18 mmol) was dissolved in a mixture of tetrahydrofuran (160 mL) and methanol (160 mL). The two solutions were then mixed in a 1000 mL flask and refluxed for 12 h at 80˚C. The mixture was cooled to room temperature, filtered and the filtrate was adjusted to a pH of 4 with 1.0 M HCl. The resulting TCPP(H2) solid was then filtered, washed with water and dried on top of a fine glass frit. This solid was then re-dissolved in tetrahydrofuran (100 mL) and precipitated by adding into hexanes (600 mL). After filtering and drying, TCPP(H2) was obtained as a fine-powder. Yield = 8.84 g (63%); ^{1}H NMR (400 MHz, dmso-d_6 as 2.50 ppm): δ 8.869 (s, 8H), 8.392 (d, 8H, J = 8.4), 8.341 (d, 8H, J = 8.0), -2.941 (s, 2H). MS (MALDI-TOF): 790.9 [$M^{\bullet+}$] (calc 791).

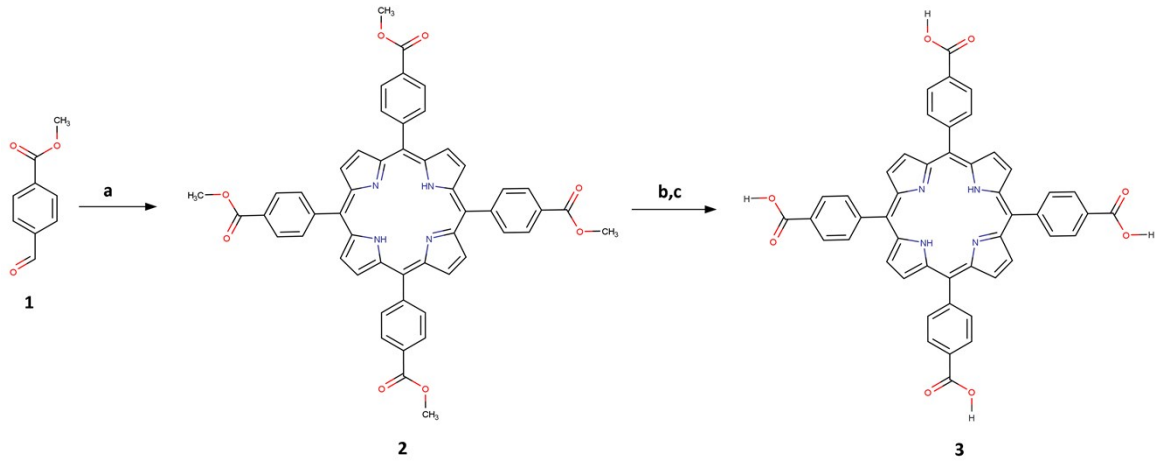

Scheme S1. Synthesis of TCPP(H2). (a) propionic acid, pyrrole, reflux 12 h in dark; (b) THF, MeOH, KOH(aq), Reflux 12 h 80°C in darkness; (c) 1M HCl (pH~4)

.

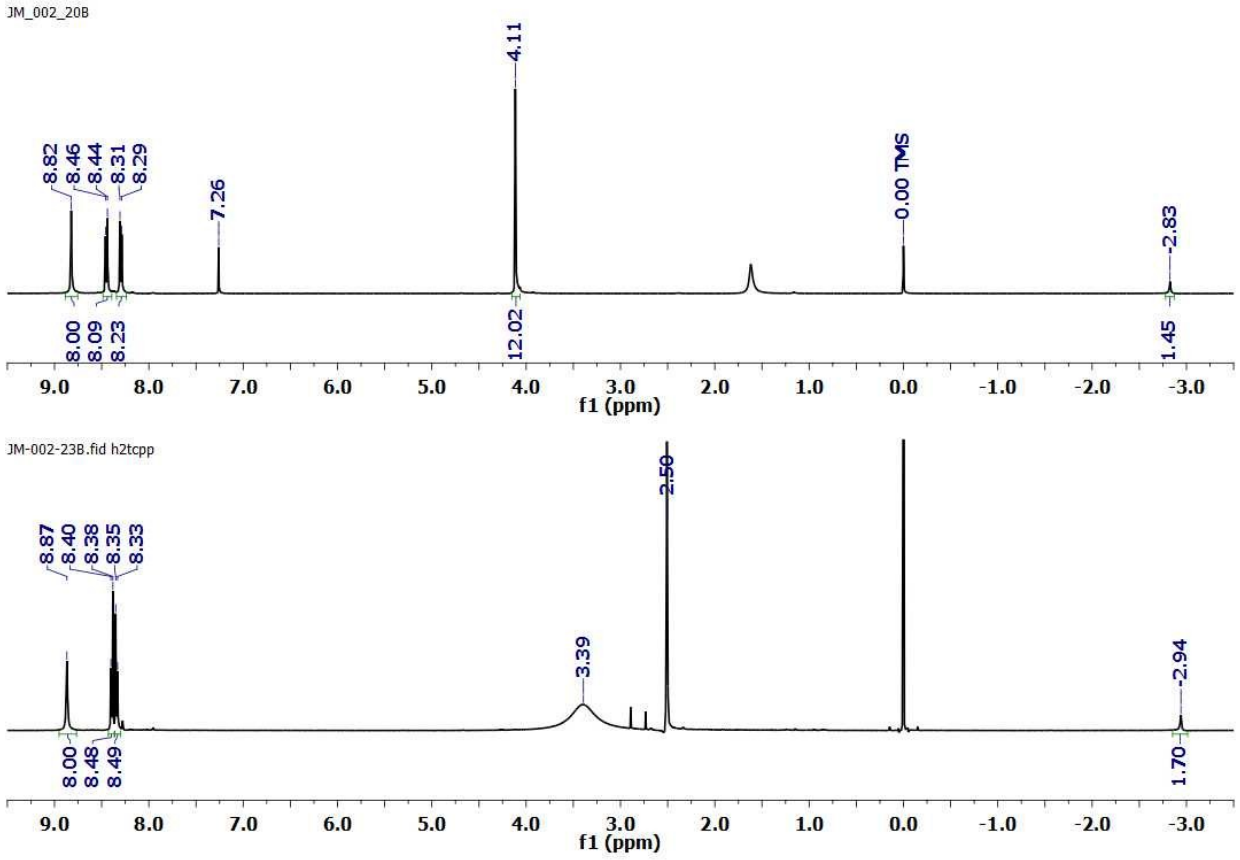

Fig. S1. ^{1}H NMR spectra of 5,10,15,20-tetrakis(4-methoxycarbonylphenyl) porphyrin, TCPPOMe(H2) (*top*) in $CDCl_3$ and 5,10,15,20-tetrakis(4-carboxyphenyl)porphyrin TCPP(H2) in DMSO-d_6 at room temperature.

C2. Synthesis of MOFs

Synthesis of NU-902

Zirconyl chloride octahydrate (25 mg; 0.075 mmol) and benzoic acid (675 mg; 5.502 mmol) were taken in a 6-dram vial and dissolved in 12 mL DMF via sonication (10 min). The resulting clear solution was incubated in an oven at 80 ºC for 105 minutes, following which it was cooled to room temperature and H_4TCPP (25 mg; 0.031 mmol) was then added. The mixture was sonicated in a bath sonicator (10 min). The resulting clear dark purple solution was heated in an oil bath at 95 ºC overnight. After cooling to room temperature and removal of the mother liquor, the microcrystalline MOF sample was centrifuged and washed with fresh DMF five times over the course of 2 days. The solid was soaked (overnight) and washed with acetone (4×15 mL), and finally dried in a vacuum desiccator (~100 torr) for 24 h; the isolated yield from three vials was ~ 100 mg.

Synthesis of PCN-222[2]

Zirconyl chloride octahydrate (97 mg; 0.30 mmol) and benzoic acid (2.7 g; 22.05 mmol) were placed in a 8-dram vial (VWR) and dissolved in 10 mL *N,N'*-diethylformamide (DEF) *via* sonication (10 min). The resulting solution was incubated in an oven at 80 ºC for 2 h, then cooled to room temperature and H_4TCPP (50 mg; 0.06mmol) and $ZnCl_2$ (~55 mg; 0.37 mmol) were added. The mixture was sonicated (10 min) forming a clear solution, which was heated in an oil bath at 120 ºC for 6 h. After cooling to room temperature and removal of the mother liquor, the microcrystalline MOF sample was centrifuged and washed with fresh DMF five times over the course of 3 days. The solid was soaked (overnight) and washed with acetone (4×15 mL), and finally dried in a vacuum desiccator (~100 torr) to yield ~70 mg of PCN-222.

For the activation involving the removal of ligated benzoates, 0.5 mL of 8 M HCl (aq) was added to a portion of isolated as-synthesized solid material (~75 mg) suspended in DMF (10 mL in total), and the resulting suspension was heated at 100 °C oven for 18-24 h (See Figures S3-S5). The suspension was then cooled to room temperature, centrifuged (5 min, 7000 rpm), and washed (3×12 mL) with fresh DMF. The residual solid was soaked (overnight), washed with acetone (4×15 mL), and finally dried in a vacuum desiccator (~100 torr) to yield ~50 mg of activated MOF.

Post-synthesis metallation of NU-902 and MOF-525**:** The Zn(II)-metallated MOF samples were prepared according to published protocol.[3] Briefly, a portion of benzoate removed NU-902 or MOF-525 was added to a zinc acetate dihydrate solution (10 mL 0.062 M in DMF) and was heated at 100 °C for 18 h with occasional swirling. The microcrystalline powder was collected by centrifugation (5 min, 7000 rpm) and washed sequentially with DMF (5×10 mL) and acetone (5×10 mL). The solvent was finally dried in a vacuum (~100 torr) at 60 °C for 24 h.

Synthesis of MOF-525[1, 4]

Zirconyl chloride octahydrate (97 mg; 0.30 mmol) and benzoic acid (2.7 g 22 mmol) were taken in a 6-dram vial and ultrasonically (10 minutes) dissolved in 8 mL DMF. The clear solution was incubated in an oven at 80 °C for 2h. After cooling down to room temperature, 47 mg (0.06 mmol) of H_4TCPP was added to this solution and the mixture was sonicated for 20 min. The purple suspension was heated at the bottom of an isotemperature gravity oven set at 70 °C for 24h. After cooling down to room temperature, the purple-red polycrystalline material was isolated by centrifugation and washed 3 times with DMF. The microcrystalline MOF sample was centrifuged and washed with fresh DMF three times followed by an exchange of acetone three times. The solid was then dried in a vacuum desiccator (~100 torr) at room temperature overnight yielding ~220 mg of MOF-525 from four vials.

D. Characterization data.

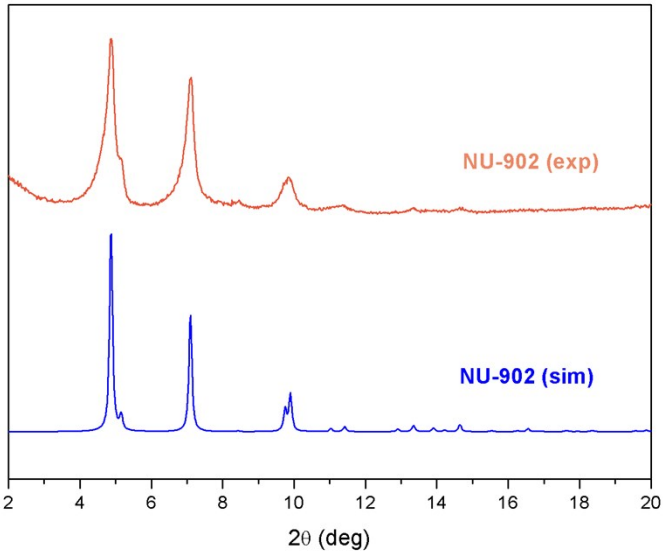

Fig. S2. PXRD patterns for NU-902(H2), showing good agreement with the simulated PXRD pattern.

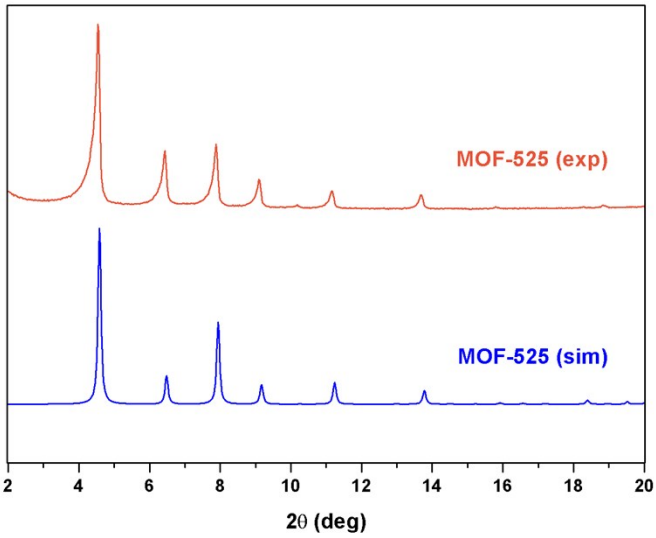

Fig. S3. PXRD patterns for MOF-525(H2) and showing good agreement with simulated patterns.

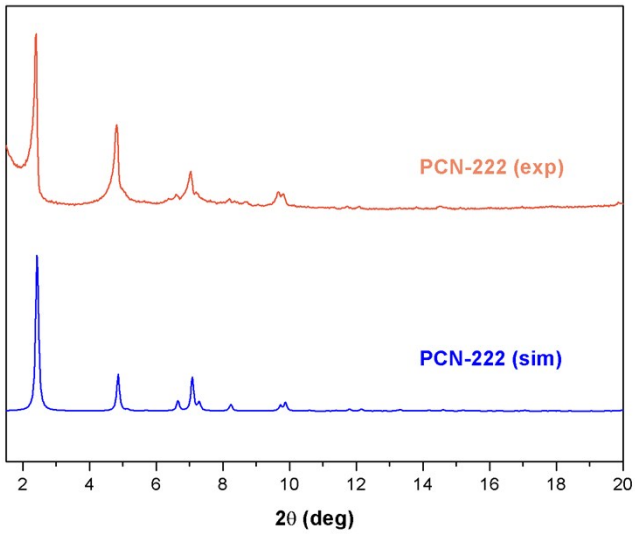

Fig. S4. PXRD patterns for PCN-222, showing good agreement with simulated patterns.

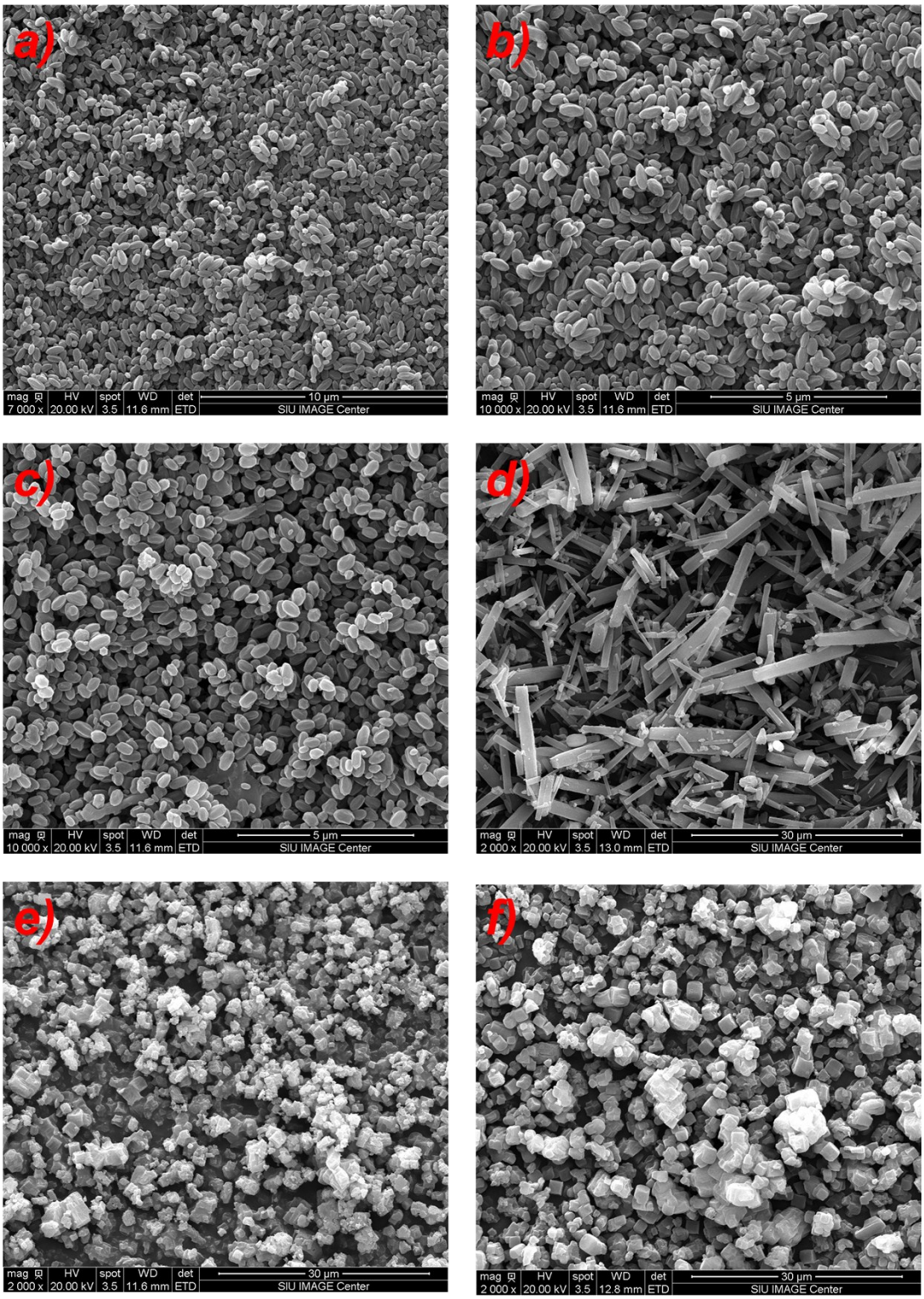

Fig. S5. SEM picture of polycrystalline MOF samples: (a-c) NU-902(H2) (from different syntheses batches), (d) PCN-222(H2), and (e, f) MOF-525(H2).

E Details of the Computational works

Linker optimization

To affirm the position of the H-atoms and to obtain the atomic coordinates of the stable conformation (instead of the thermally allowed probable coordinates) of linkers, required for computing the electronic transitions, DFT optimizations within the framework connectivity were performed. In order to perform computationally affordable quantum mechanics calculations, we truncated the number of atoms involved in the simulation. Coordinates of the two adjacent 'dimeric' Por-M units with the smallest torsional angle were extracted with Zr_6-oxo clusters removed. These structures were optimized with the carboxylate ($-CO_2$) moieties kept fixed at positions with their corresponding crystallographic coordinates, where all other atoms were allowed to relax during optimization. Note that optimization was performed on the carboxylic acid form after protonating the carboxylates. The density functional theory calculations were done using the Gaussian 09[5] software with a hybrid exchange-correlation functional CAM-B3LYP[6] combining the three-parameter Becke gradient-corrected exchange functional[7] with the Lee-Yang-Parr correlation functional (B3LYP)[8] and long-range correction using the Coulomb-Attenuating method in conjunction with the LANL2DZ basis set.[9] The self-consistent field convergence criterion was set to 10^{-8}. The monomeric TCPP(H2) and TCPP(Zn) were optimized unconstrained.

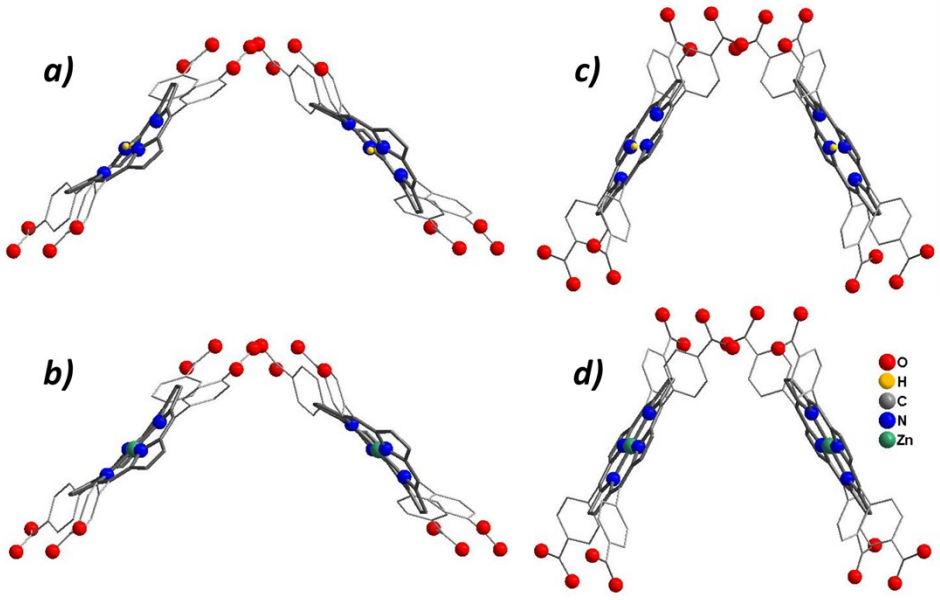

Fig. S6. DFT optimized structures of closely positioned porphyrin dimers in (*a, b*) MOF-525 [90°, $d_{M\text{-}M}$ = 13.5Å] and (*c, d*) NU-902 [60°, $d_{M\text{-}M}$ = 10.5Å]; M = H2 or Zn; H atoms connected to C and O are omitted for clarity.

UV/VIS spectra calculation

UV/VIS spectra were computed for the DFT optimized monomeric TCPP(H2) and TCPP(Zn) and 'dimeric' linkers using time-dependent DFT approach (TD-DFT) implemented in Gaussian 09.[5] The calculations were done using the CAM-B3LYP functional in conjunction with the LANL2DZ basis set. The self-consistent field convergence criterion was set to 10^{-8}. In our calculations, fifteen singlet excited states were considered for solution. From this procedure, electronic transitions, vertical excitation energies, absorbance wavelengths, and oscillator strengths were obtained and are tabulated in **Table S1**.

The corresponding absorption spectra were simulated via a Gaussian reconvolution with FWHM = 800 cm^{-1} and plotted in **Fig. 3** and **Fig. S8b** around the wavelength positions corresponding to the computed electronic transitions using the corresponding oscillator strength. Molecular orbitals involved in the most relevant electronic transitions were visualized via the Gaussview software[10] with isovalues of 0.02 electrons per cubic atomic unit, which are shown in **Fig. S7**.

Table S1. Selected TD-DFT computed transitions for monomeric TCPP(H2), TCPP(Zn), and 'dimeric' **NU-902(H2)** and **NU-902(Zn)** linkers. (H = HOMO and L = LUMO)

Species	Excited state	Transition energy (eV)	Wavelength (nm)	Oscillator Strength	MOs involved in the transitions
TCPP(H2)	1	2.090	593.3	0.03	H-1→L+1 (36%); H→L (63%)
	2	2.329	532.4	0.05	H→L+1 (60%); H-1→L (39%)
	3	3.349	370.3	1.43	H→L (31%); H-1→L+1 (59%)
	4	3.435	360.9	1.92	H→L+1 (40%); H-1→L (59%)
NU-902(H2) ['dimer']	1	2.074	598.0	0.001	H-3→L+1 (11%); H-2→L+3 (18%); H-1 →L (16%); H→L+2 (26%)
	2	2.079	597.0	0.060	H-3→L+1 (18%); H-2→L+3 (13%); H-1 →L (33%); H→L+2 (23%)
	3	2.308	537.2	0.032	H-3→L (17%); H-2→L+2 (13%); H-1 →L+1 (25%); H→L+3 (19%)
	4	2.314	535.9	0.083	H-3→L (14%); H-2→L+2 (18%); H-1 →L+1 (24%); H→L+3 (31%)
	5	3.263	380.0	0.004	H-3→L+1 (26%), H-2→L+3 (24%), H-1→L (12%) H→L+2 (9%)
	6	3.315	374.0	1.223	H-3→L (25%), H-2→L+2 (21%), H-1→L+1 (15%), H→L+3 (13%)
	7	3.346	370.5	2.608	H-3→L+1 (24%), H-2→L+3 (26%), H-1→L (15%), H→L+2 (14%)
	8	3.433	361.2	2.780	H-3→L (23%), H-2→L+2 (25%), H-

					1→L+1 (19%), H→L+3 (19%)
TCPP(Zn)	1	2.317	535.1	0.005	H-1→L (45%), H→L+1 (54%)
	2	2.317	535.1	0.005	H→L (54%), H-1→L+1 (45%)
	3	3.495	354.8	1.71	H→L (44%), H-1→L+1 (54%)
	4	3.495	354.8	1.71	H-1→L (45%), H→L+1 (54%)
NU-902(Zn) [‘dimer’]	1	2.257	549.3	0.012	H-3→L (10%), H-2→L+2 (10%), H-1→L+1 (15%), H→L+2 (10%), H→L+3 (14%)
	2	2.258	549.0	0.003	H-3→L+1 (10%), H-2→L+3 (13%), H-1→L (10%), H→L+2 (13%)
	3	2.260	548.5	0.042	H-3→L (12%), H-2→L+2 (14%), H-1→L+1 (20%), H→L+3 (23%)
	4	2.263	548.0	0.051	H-3→L+1 (16%), H-2→L+3 (14%), H-1→L (22%), H→L+2 (19%)
	5	3.305	375.1	1.15	H-3→L (22%), H-2→L+2 (19%), H-1→L+1 (15%), H→L+3 (14%)
	6	3.314	374.1	0.011	H-3→L+1 (24%), H-2→L+3 (22%), H-1→L (14%), H→L+2 (10%)
	7	3.411	363.4	3.070	H-3→L+1 (19%), H-2→L+3 (21%), H-1→L (17%), H→L+2 (16%)
	8	3.421	362.4	2.885	H-3→L (19%), H-2→L+2 (21%), H-1→L+1 (17%), H→L+3 (18%)

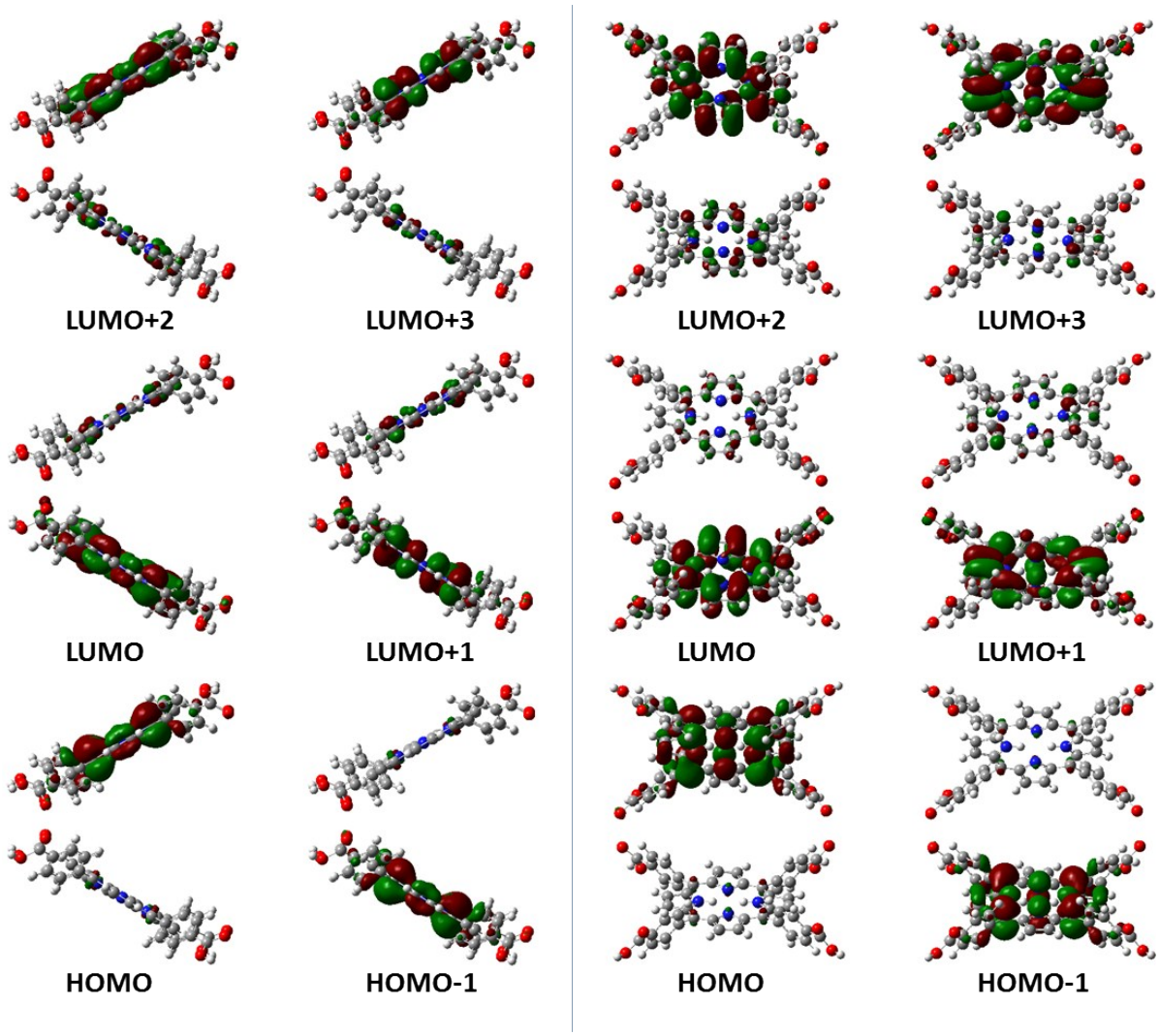

Fig. S7. Frontier molecular orbitals of the NU-902(H2) [dimer] (left) side and (right) front view highlighting shared electronic density in the FMOs due to strong interaction.

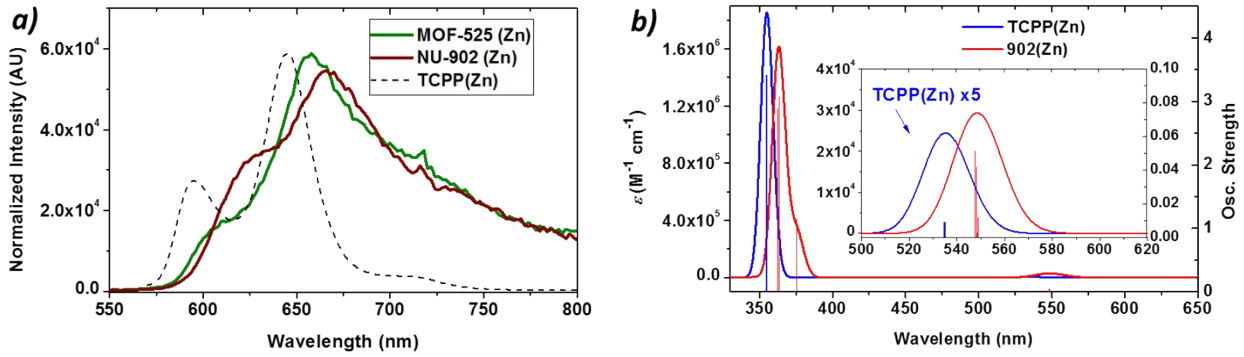

Fig. S8. Steady state (*a*) emission spectra for NU-902(Zn) and MOF-525(Zn); the dashed line represents spectrum for free TCPPOMe(Zn) linker for comparison. *b*) TDDFT computed electronic spectra of TCPP(Zn) and for dimeric TCPP(Zn) of NU-902(Zn) shown in Fig. S6d; the inset displays a magnification of the spectral window near the Q-band region.

F. Spectroscopic data.

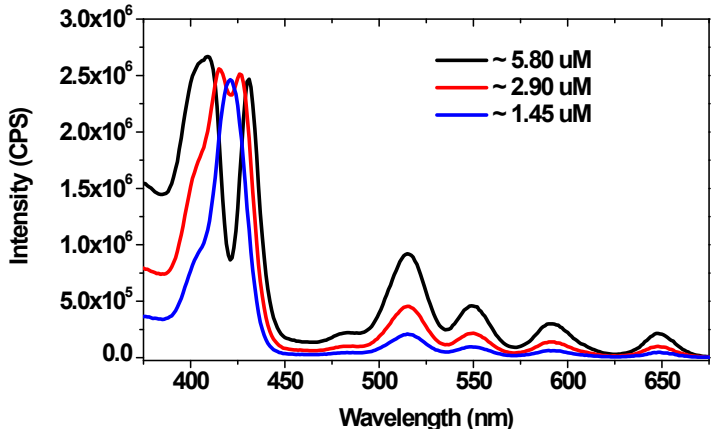

Fig. S9. Steady state excitation spectra for free TCPPOMe(H2) probed at the lowest $Q_{0,1}$ band (715 nm) at different noted concentrations indicating aggregation mediated spectral evolution: a Soret band split and relatively higher contribution for the Q-band transitions can be observed at higher concentration.

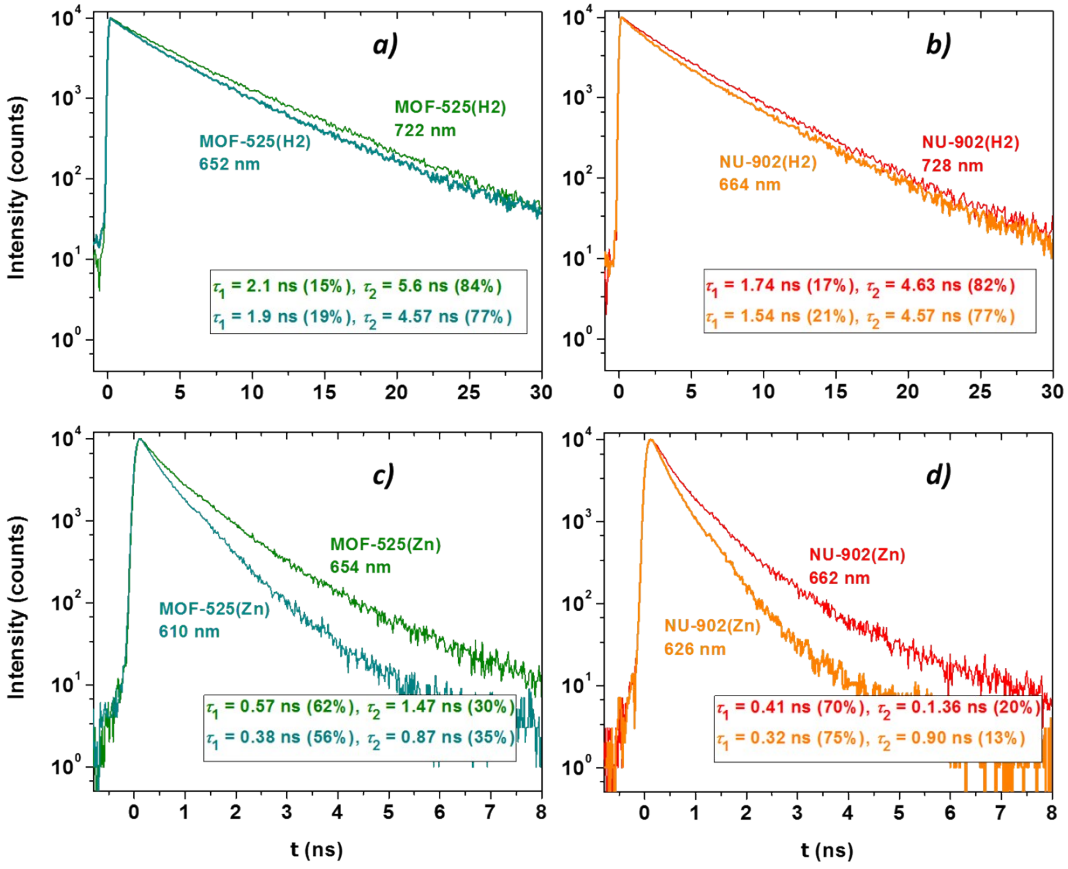

Fig. S10. Transient emission decay profile for (*a, b*) free-base and (*c, d*) zinc(II) metallated NU-902 and MOF-525 at $Q_{0,0}$ and $Q_{0,1}$ bands.

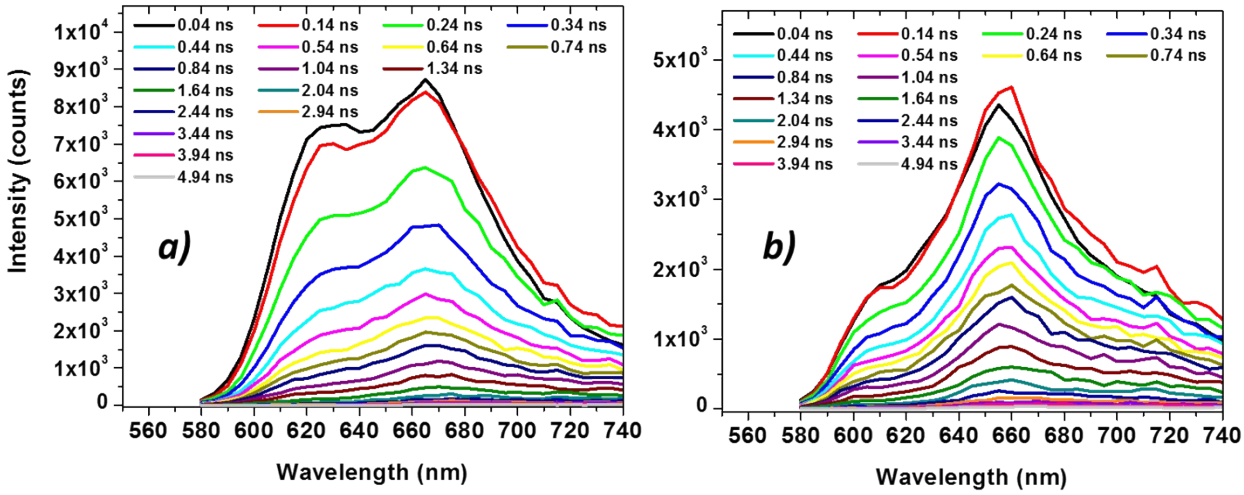

Fig. S11. Time resolved emission spectra for (*a*) NU-902(Zn) and (*b*). MOF-525(Zn).

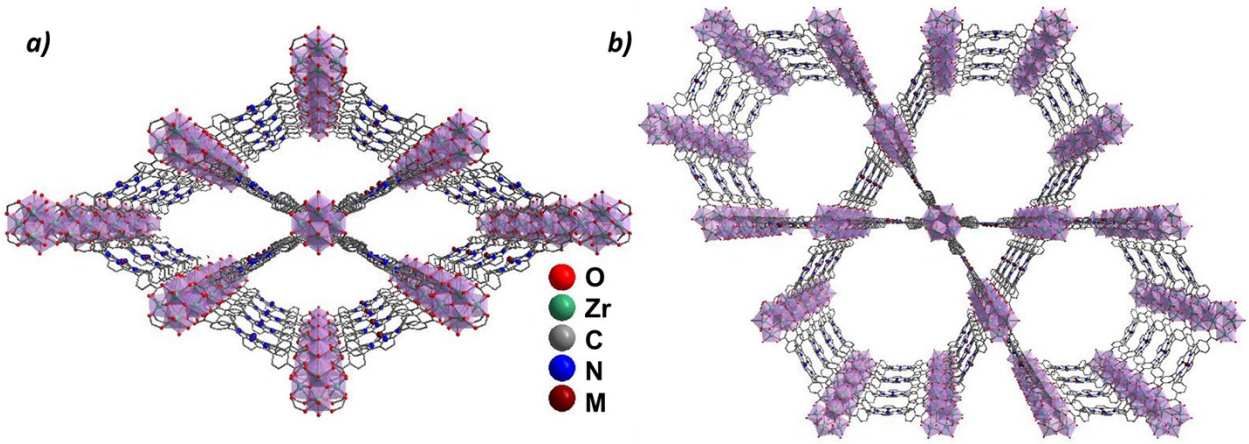

Fig. S12. Molecular structures of porphyrin-based MOFs (*a*) NU-902 and (*b*) PCN-222.

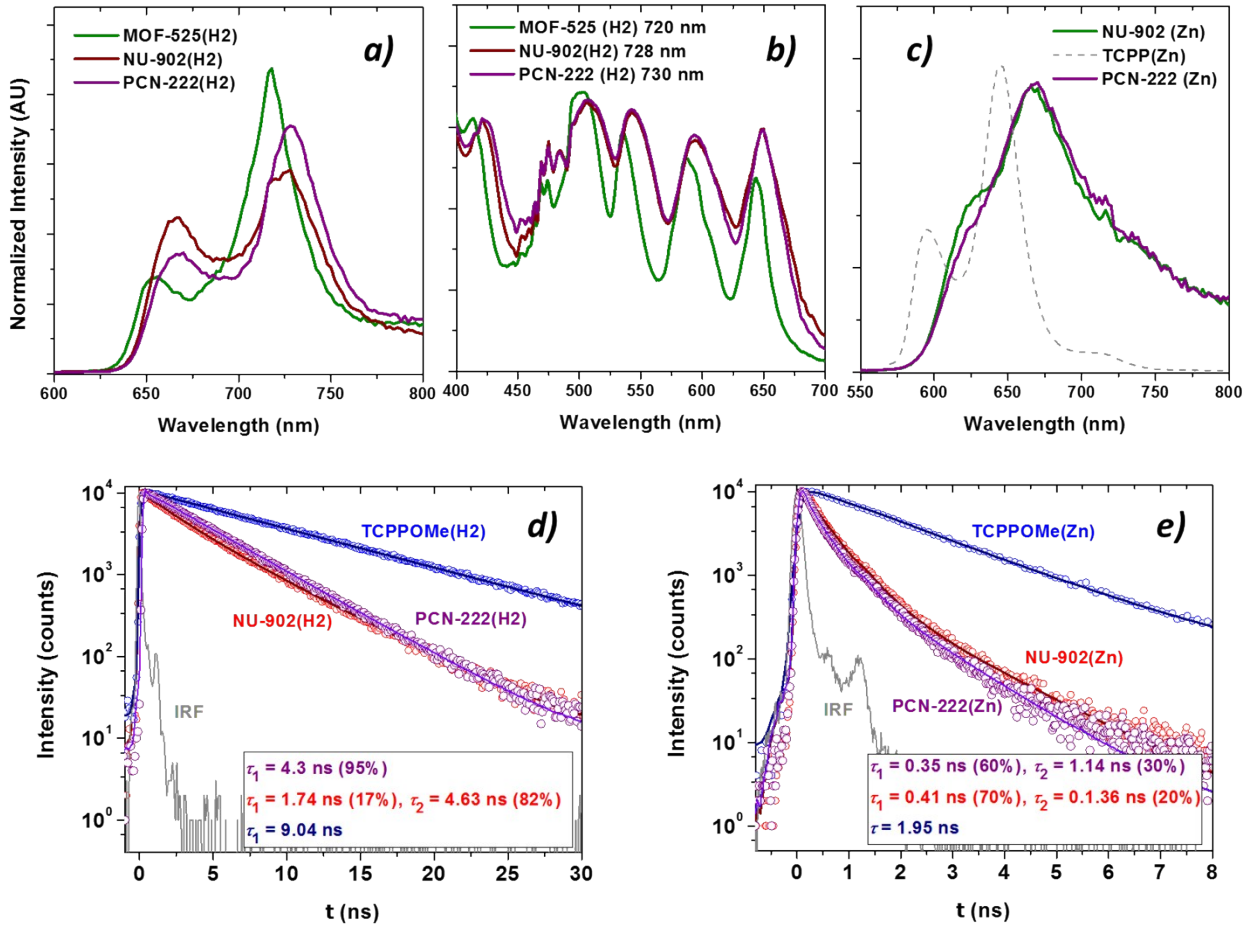

Fig. S13. The similarity of emissive spectral features among the PCN-222 and NU-902 samples: (*a, c*) steady state emission and (*b*) excitation spectra for NU-902 and PCN-222. c) Time-resolved emission spectra for (*d*) PCN-222(H2) and (e) PCN-222(Zn) with corresponding NU-902 samples.

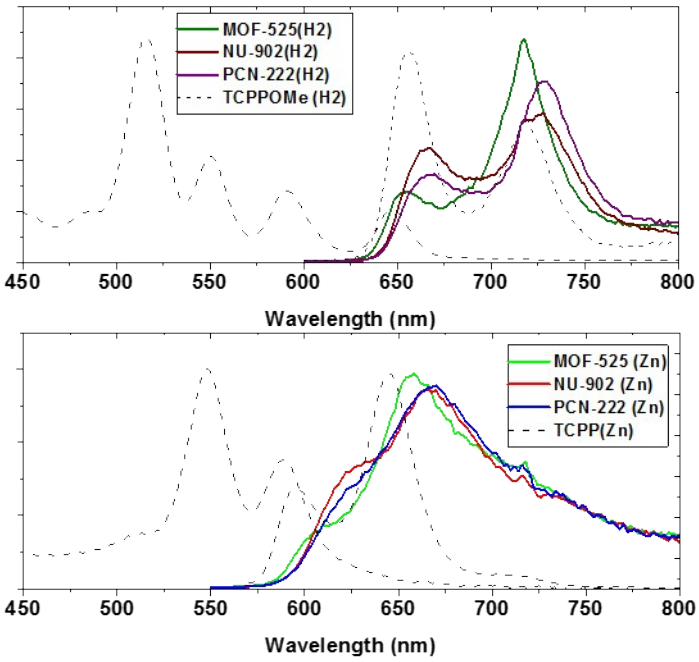

Fig. S14. Steady-state emission spectra of (*a*) free-base and (*b*) zinc(II)-metallated samples are plotted against the corresponding free linker absorption spectra (dashed gray) to qualitatively access the overall poor spectral overlap. Note a quantitative evaluation would be possible with the exact absorption spectra of the solid MOF samples.

G. Quenching experiments

In order to study the efficiency of singlet state energy transfer process within some of these MOF samples, we performed the amplified photoluminescence quenching. For that, we installed ferrocene (Fc) based **Fc-COO⁻** quencher *via* a well-established solvent assisted ligand incorporation (SALI; **Scheme S2**) method at the Zr_6-oxo node.[11] Contrary to usual techniques, where quenchers have been introduced in solution or *via* thermally labile coordination to under-coordinated metal centers, SALI involves an acid-base reaction between an incoming Fc-COOH ligand with the hydroxy and aqua ligands at the 8-connected Zr_6 nodes of NU-902. Thus SALI[11a, 11b] offers a novel route to homogeneously install fluorescence quencher *via* $Zr^{(IV)}$–carboxylate linkage.

We implemented SALI to prepare Fc –doped NU-902 samples following published procedure.[11b-11d, 12] In brief, a 15 mg portion of activated pristine **NU-902** (0.0063 mmol) was soaked in solutions containing various concentration of Fc-COOH (where the sum of Fc-COOH and benzoic acids are 0.0063 mmol) in 10 mL vials, which was then capped and heated at 60 °C for 24 h with occasional swirling. The supernatant of the reaction mixture was decanted and the MOF sample was soaked, centrifuged and washed with fresh DMF five times over the course of 2 days. The solid was soaked (overnight) and washed with acetone (4×15 mL), and finally dried in a vacuum desiccator (~100 torr). The loadings of Fc-COO⁻ at the node were determined via SEM-EDS elemental analysis and corroborated with ICP-MS data.

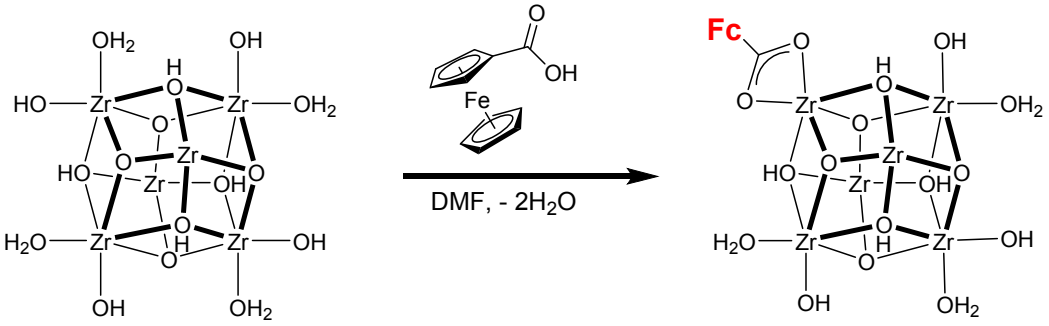

Scheme S2. Installation of **Fc-COO⁻** in NU-902 *via* SALI (showing a maximum targeted loading for 1:1 Fc/Por).

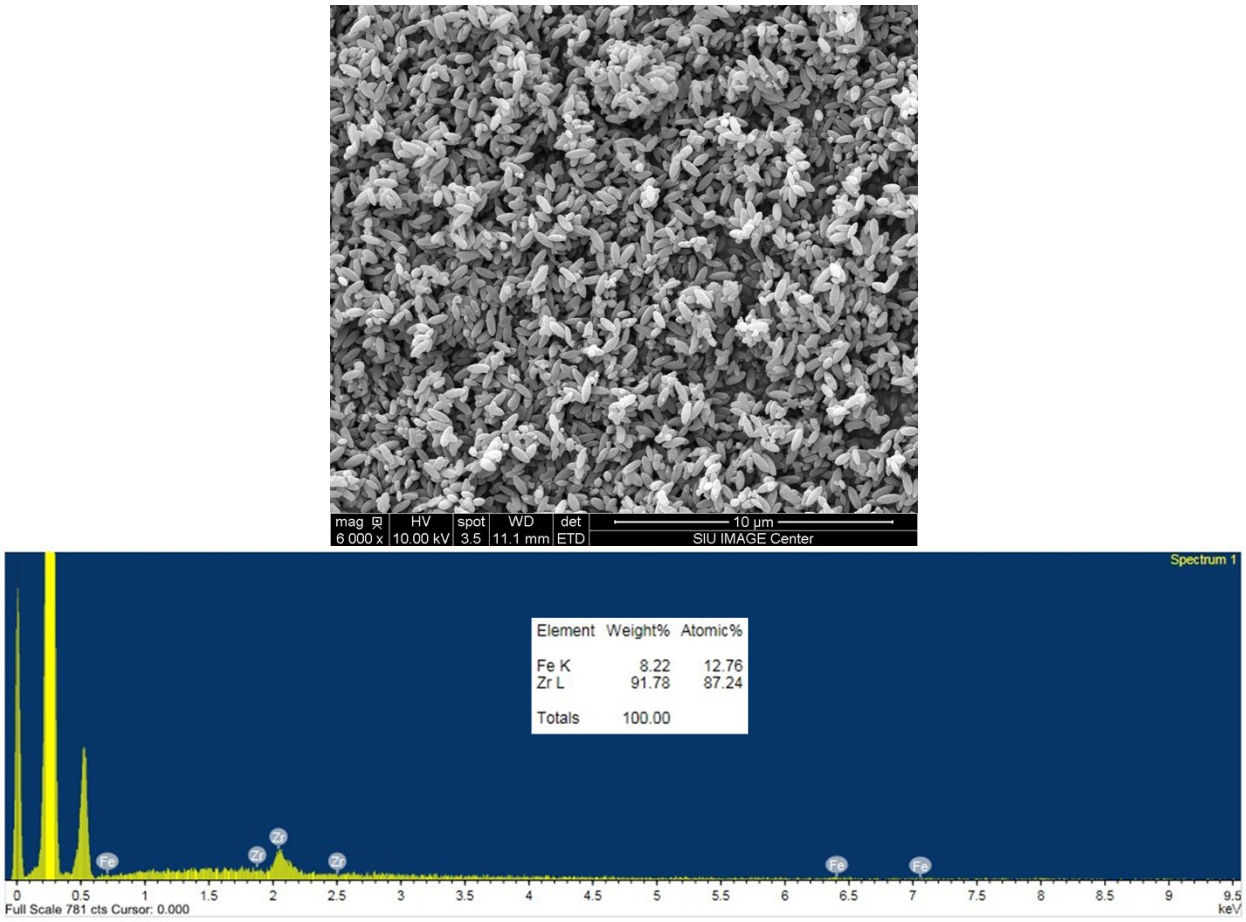

Fig. S15. SEM picture of one of the **Fe-COO** doped NU-902(H2) (*top*) sample and the EDS spectrum (*bottom*) of the same; (inset showing Fe/Zr atom ratio).

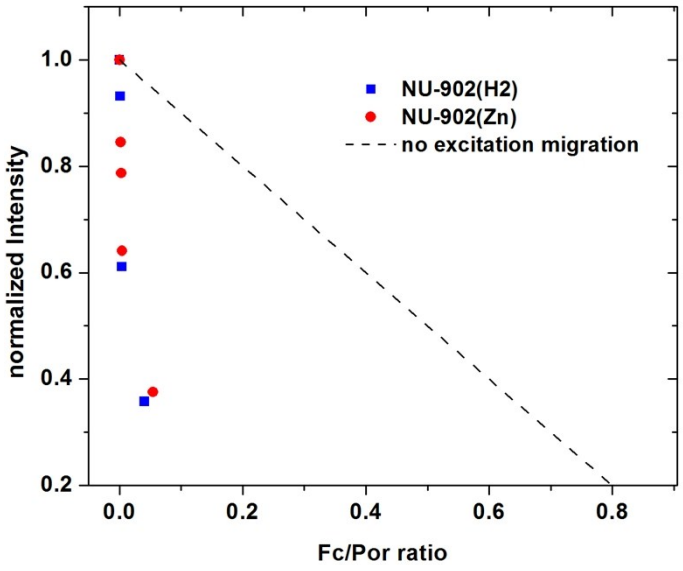

Fig. S16. Steady-state emission intensities of NU-902(H2) and NU-902(Zn) with respect to the extent of **Fc-COO** loading (Fc/por: 0 to 1). The dashed gray line simulates the behavior expected when exciton migration is absent (i.e. quenching for only 1:1 complex)

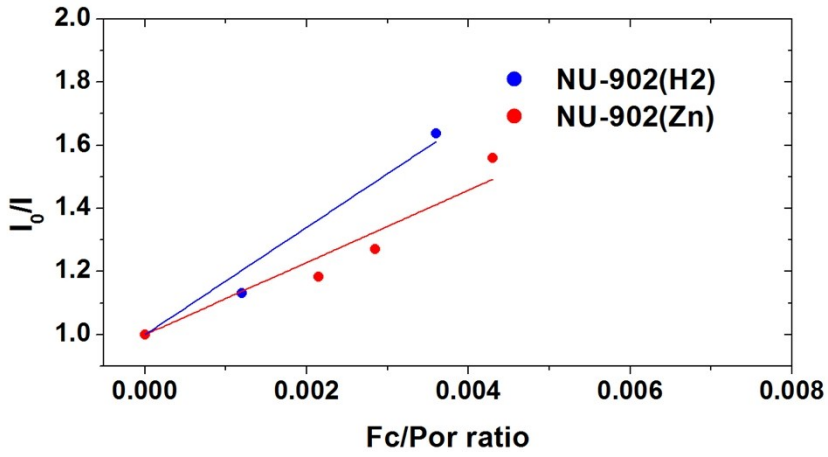

Fig. S17. Stern-Volmer plots for free-base and zinc(II) metallated NU-902 samples doped with various degree of **FcCOO** quencher.

With **Fc-COO⁻** installed at various Fc/por doping ratio, **Fig. S16** highlights an amplified emission quenching, which was analyzed using Stern-Volmer relationship,

$$\frac{I_0}{I} = 1 + K_{SV}[FcCOO] \qquad (1)$$

where I_0 and I are the fluorescence intensity without and with a quencher at a particular level of the quencher. **Fig. S17** highlights the SV-fitting curve for NU-902(H2) and NU-902(Zn). With quenchers directly attached to the MOF, the slope K_{SV} represents the number of chromophores the exciton visits within its lifetime; fit of the experimental data yield a slope of 170 for NU-902(H2) and 114 for NU-902(Zn) which is the number of chromophores the exciton visits within its lifetime and these are 170 for NU-902(H2) and 114 for NU-902(Zn) with corresponding absolute displacement estimated to be 85 and 57 linkers respectively. The number of hops made by the exciton is $(85)^2$ or about 7224 for NU-902(H2) and 3249 for NU-902(Zn), with estimated hopping times of 4630/7225 = 0.65 ps and 410/3249 = 0.13 ps, respectively.

Considering the saturation emission intensity at 0.040 and 0.055 of Fc/por doping level (**Fig. S16**), we estimated electron transfer rate using the following equation:

$$\frac{I_0}{I_s} = 1 + \tau_0 k_e$$

Where τ_0 is the intrinsic fluorescence lifetime without Fc-quencher and k_e is the electron transfer rate from the Fc to porphyrin , which was estimated to be at least ~0.4×10^9 s^{-1} for NU-902(H2) and ~4×10^9 s^{-1} for NU-902(Zn). These metrics are in agreement to the related 5,15-dipyridyl(porphinato)zinc(II) based MOF.[13]

MOF-525 consists of a saturated [12,4] connected node and does not possess labile terminal hydroxyl and aqua ligands suitable for a carboxylate attachment. However, taking advantage of few defect sites to install Fc-COO^- we roughly estimated a similar number of exciton hopping during its lifetime in comparison to the NU-902 system. However, it should be noted that without the knowledge of exact defect density, the exact Fc/Por number may not be very precise.

H. References

1. Z. Q. Wang, B. X. Wang, Y. Yang, Y. J. Cui, Z. Y. Wang, B. L. Chen and G. D. Qian, *Acs Applied Materials & Interfaces*, 2015, **7**, 20999-21004.
2. D. W. Feng, Z. Y. Gu, J. R. Li, H. L. Jiang, Z. W. Wei and H. C. Zhou, *Angewandte Chemie-International Edition*, 2012, **51**, 10307-10310.
3. W. Morris, B. Volosskiy, S. Demir, F. Gándara, P. L. McGrier, H. Furukawa, D. Cascio, J. F. Stoddart and O. M. Yaghi, *Inorg. Chem.*, 2012, **51**, 6443-6445.
4. I. Hod, M. D. Sampson, P. Deria, C. P. Kubiak, O. K. Farha and J. T. Hupp, *ACS Catalysis*, 2015, **5**, 6302-6309.
5. M. J. Frisch, G. W. Trucks, H. B. Schlegel, G. E. Scuseria, M. A. Robb, J. R. Cheeseman, G. Scalmani, V. Barone, B. Mennucci, G. A. Petersson, H. Nakatsuji, M. Caricato, X. Li, H. P. Hratchian, A. F. Izmaylov, J. Bloino, G. Zheng, J. L. Sonnenberg, M. Hada, M. Ehara, K. Toyota, R. Fukuda, J. Hasegawa, M. Ishida, T. Nakajima, Y. Honda, O. Kitao, H. Nakai, T. Vreven, J. A. Montgomery, Jr., J. E. Peralta, F. Ogliaro, M. Bearpark, J. J. Heyd, E. Brothers, K. N. Kudin, V. N. Staroverov, R. Kobayashi, J. Normand, K. Raghavachari, A. Rendell, J. C. Burant, S. S. Iyengar, J. Tomasi, M. Cossi, N. Rega, M. J. Millam, M. Klene, J. E. Knox, J. B. Cross, V. Bakken, C. Adamo, J. Jaramillo, R. Gomperts, R. E. Stratmann, O. Yazyev, A. J. Austin, R. Cammi, C. Pomelli, J. W. Ochterski, R. L. Martin, K. Morokuma, V. G. Zakrzewski, G. A. Voth, P. Salvador, J. J. Dannenberg, S. Dapprich, A. D. Daniels, Ö. Farkas, J. B. Foresman, J. V. Ortiz, J. Cioslowski and D. J. Fox, *Gaussian 09*, Revision D.01. Gaussian Inc., Wallingford CT, 2009
6. T. Yanai, D. P. Tew and N. C. Handy, *Chem. Phys. Lett.*, 2004, **393**, 51-57.
7. A. D. Becke, *J. Chem. Phys.*, 1993, **98**, 1372.
8. C. Lee, W. Yang and R. G. Parr, *Phys. Rev. B: Condens. Matter*, 1988, **37**, 785.
9. T. H. Dunning Jr and P. J. Hay, *Modern Theoretical Chemistry*, Plenum New York, 1977.
10. R. Dennington, T. Keith and J. Millam, *GaussView*, 3. Semichem Inc., Shawnee Mission, KS, 2009
11. (a) I. Hod, O. K. Farha and J. T. Hupp, *Chem. Commun.*, 2016, 1705-1708; (b) P. Deria, W. Bury, I. Hod, C.-W. Kung, O. Karagiaridi, J. T. Hupp and O. K. Farha, *Inorg. Chem.*, 2015, **54**, 2185-2192; (c) P. Deria, W. Bury, J. T. Hupp and O. K. Farha, *Chem. Commun.*, 2014, **50**, 1965-1968; (d) P. Deria, J. E. Mondloch, E. Tylianakis, P. Ghosh, W. Bury, R. Q. Snurr, J. T. Hupp and O. K. Farha, *J. Am. Chem. Soc.*, 2013, **135**, 16801-16804.
12. P. Deria, Y. G. Chung, R. Q. Snurr, J. T. Hupp and O. K. Farha, *Chem. Sci.*, 2015, DOI: 10.1039/c1035sc01784j.

13. H.-J. Son, S. Jin, S. Patwardhan, S. J. Wezenberg, N. C. Jeong, M. So, C. E. Wilmer, A. A. Sarjeant, G. C. Schatz, R. Q. Snurr, O. K. Farha, G. P. Wiederrecht and J. T. Hupp, *J. Am. Chem. Soc.*, 2013, **135**, 862-869.